Analysis of a wavelet arising from a model for arm movements during epileptic seizures

T.M.E. Nijsen, A.J.E.M Janssen, *Fellow IEEE*, and R.M. Aarts, *Fellow IEEE*

***Abstract*— This paper analyses a wavelet that arises in the study of myoclonic seizures. The wavelet comes about when a physiological model is used that describes arm movements associated with certain epileptic (myoclonic) seizures. Due to the simple analytical form of the wavelet, $x(t) = 0$ for $t < 0$ and $x(t) = te^{-t} - \frac{t}{A}e^{\frac{-t}{B}}$ for $t \geq 0$, with $B^2 \approx A \approx 1$, explicit computations are feasible for the frequency response $X(\omega)$, the admissibility condition and admissibility constant, the wavelet transform of x itself using x or its time-reversed version x_- (matched filter) as analyzing wavelet, etc. The new wavelet is expected to yield better detectability for the problem at hand than general purpose wavelets would do. We show one example of how the new wavelet performs on clinical data and we intend to follow up this study with a more elaborate demonstration of its efficacy. The new wavelet, and some of its variants (such as the odd extension of it and a Gaussian smoothed version of it), are briefly compared with certain wavelets presented in existing literature. Our preliminary conclusion, to be elaborated in the near future, is that the wavelet has excellent potential in the detection of myoclonic seizures from accelerometric data of arm movements of epileptic patients.**

***Index Terms*— accelerometry, epilepsy, myoclonic seizure, wavelet**

I. Introduction

In this paper a wavelet is analysed that arises from an analytical model for accelerometric output associated with myoclonic seizures. This wavelet can be used to derive salient features of myoclonic seizure waveforms from accelerometric data. Figure 1 shows two typical examples of an accelerometer pattern associated with a myoclonic seizure. A myoclonic seizure consists of one single muscle jerk. The electrical activation of the muscle lasts less than 50 milliseconds [1]. Both the agonists and the antagonists in the muscle groups involved contract and relax synchronously.

The clinical manifestation of myoclonic seizures is very subtle so that they are often missed by current available detection systems. Detecting these subtle seizures is of clinical importance. A patient can experience many myoclonic seizures during the night that can disturb sleep rhythm. Counting myoclonic seizures may also be an important measure for successful medical treatment. Furthermore, severe motor seizures are often preceded by myoclonic seizures, so that detection of myoclonic seizures could be used for early warning.

T.M.E. Nijsen is with the Eindhoven University of Technology, Eindhoven, The Netherlands and Kempenhaeghe Epilepsy Centre, Heeze, The Netherlands (e-mail: nijsent@kempenhaeghe.nl)

A.J.E.M. Janssen is with Philips Research Laboratories, Eindhoven, The Netherlands

R.M. Aarts is with Philips Research Laboratories, Eindhoven, The Netherlands and the Eindhoven University of Technology, Eindhoven, The Netherlands

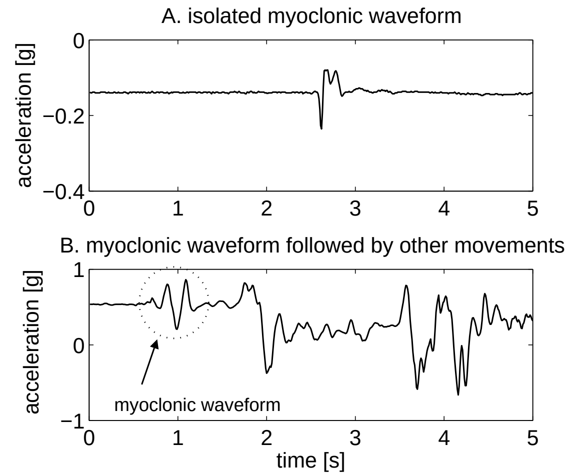

Fig. 1. Examples of accelerometric waveforms associated with myoclonic seizures.

In choosing suitable features for automated detection of these seizures from the ACM-signal, knowledge about these patterns is important. Previously we presented an analytical model that describes the accelerometric output during a myoclonic seizure [2]. In this paper this model is used to derive a matched wavelet transform.

In [2] signals of the form

$$\left(te^{-t/\tau} - \frac{1}{A}te^{-t/(B\tau)}\right)\chi_{[0,\infty)}(t) \ ,t \in \mathbb{R}, \tag{1}$$

are derived from a model for accelerometric patterns associated with myoclonic seizures. In Eq. 1, $\chi_{[0,\infty)}(t) = 0$ for $t < 0$ and $\chi_{[0,\infty)}(t) = 1$ for $t \geq 0$. The parameters A and B are positive, and so is τ. In particular the case is considered when $A \approx B^2$. In the case that $A = B^2$, the signal in Eq. 1 is admissible [3], [4] as a wavelet since then

$$\int_0^\infty \left(te^{-t/\tau} - \frac{1}{A}te^{-t/(B\tau)}\right) dt = \tau^2\left(1 - \frac{B^2}{A}\right) = 0. \tag{2}$$

Observe that

$$te^{-t/\tau} - \frac{1}{A}te^{-t/B\tau} = \tau\left(t'e^{-t'} - \frac{1}{A}t'e^{-t'/B}\right) \ , \ t' = t/\tau, \tag{3}$$

hence for computation purposes we may suppose $\tau = 1$. Thus the signals

$$x_{A,B}(t) := \left(te^{-t} - \frac{1}{A}te^{-t/B}\right)\chi_{[0,\infty)}(t) \ ,t \in \mathbb{R}, \tag{4}$$

are considered, and the admissible cases

$$x_C(t) := \left(te^{-t} - C^2te^{-Ct}\right)\chi_{[0,\infty)}(t) \ ,t \in \mathbb{R}. \tag{5}$$

II. Wavelet characteristics

A. Normalization and approximation by admissible wavelet

We want to approximate a general $x_{A,B}$ by an admissible x_C. To that end

$$\int_0^\infty (x_{A,B}(t) - x_{D^{-1}}(t))^2 dt \quad (6)$$

is minimized ($D = C^{-1}$). We compute

$$\int_0^\infty (x_{A,B}(t) - x_{D^{-1}}(t))^2 dt = \frac{1}{4B}\left[s^2 - \frac{16sx}{(1+x)^3} + \frac{1}{x}\right] \ , \\ s = \frac{B^2}{A} \approx 1 \ , \ x = \frac{D}{B} \approx 1 \ . \quad (7)$$

There is the Taylor expansion

$$s^2 - \frac{16sx}{(1+x)^3} + \frac{1}{x} = \\ (s-1)^2 + \sum_{l=1}^{\infty}(1-x)^l\left\{\frac{(l+1)(l-2)}{2^l}s + 1\right\} = \\ (s-1)^2 + (x-1)(s-1) + (x-1)^2 \\ -(x-1)^3(\frac{1}{2}s+1) + (x-1)^4(\frac{5}{8}s+1) + \dots \ . \quad (8)$$

The leading quadratic form in the last member of Eq. 8 can be written as

$$\left(x - 1 + \frac{s-1}{2}\right)^2 + \frac{3}{4}(s-1)^2 \quad (9)$$

and is minimal $\frac{3}{4}(s-1)^2$ when $x = \frac{3-s}{2}$. We are thus led to take $x = \frac{3-s}{2}$. Assuming A and B are known, we now have an expression for D (and C). Hence, we have an approximation x_C of $x_{A,B}$.

B. Computations for x_C

In this section an overview is given of some characteristics of x_C.

1) Energy: The energy $\|x_C\|^2$ is

$$\|x_C\|^2 = \int_0^\infty (te^{-t} - C^2te^{-Ct})^2 dt = (1-C)^2\frac{1+6C+C^2}{4(1+C)^3} \ . \quad (10)$$

2) Fourier transform: The Fourier transform $X_C(\omega)$ of x_C is given by:

$$\begin{aligned} X_C(\omega) &= \int_0^\infty (te^{-t} - C^2te^{-Ct})e^{i\omega t}dt \\ &= \left(\frac{1}{1-i\omega}\right)^2 - \left(\frac{C}{C-i\omega}\right)^2 \\ &= -2i\omega(1-C)\frac{C - \frac{1}{2}i\omega(1+C)}{(1-i\omega)^2(C-i\omega)^2} \ . \end{aligned} \quad (11)$$

Observe that $X_C(\omega) = 0$ at $\omega = 0$, which again shows that x_C is an admissible wavelet.

3) Admissibility constant: The admissibility constant C_{x_C} is computed as

$$\begin{aligned} C_{x_C} &= \int_{-\infty}^{\infty} |X_C(\omega)|^2 \frac{d\omega}{|\omega|} \\ &= \left(\frac{1-C}{1+C}\right)^2 \left\{2 - (1+4C+C^2)\frac{lnC^2}{1-C^2}\right\} \ . \end{aligned} \quad (12)$$

This admissibility constant is required when one wants to invert the wavelet transform

$$f(\tau) \to CWT_{x_C}[f](t,a) = \frac{1}{\sqrt{a}}\int_{-\infty}^{\infty} f(\tau)x_C\left(\frac{t-\tau}{a}\right)d\tau \quad (13)$$

according to the inversion formula

$$f(\tau) = \frac{1}{C_{x_C}}\int_0^\infty \int_{-\infty}^{\infty} CWT_{x_C}[f]\left(\frac{\tau - t}{a}\right)\frac{da\,dt}{a^2\sqrt{a}} \ . \quad (14)$$

4) Vanishing moments: A further issue in Wavelet analysis is the desirability of vanishing moments. We compute for $k = 0, 1, \dots$

$$\int_0^\infty t^k x_C(t)dt = (k+1)!\left(1 - \frac{1}{C^k}\right) \ ; \quad (15)$$

when $k = 0$ this vanishes for all C. When $k = 1, 2, ..$ this vanishes only when $C = 1$. In the latter case we have $x_{C=1} \equiv 0$. Therefore, except in the trivial case C=1, only the 0^{th} moment vanishes.

C. Limiting case $C \to 1$

As said, we have $x_C = 0$ when $C = 1$. Experimental evidence [5] shows that $C \approx 1$, hence we consider the renormalized wavelet $\frac{1}{1-C}x_C$, and in particular, its limit when $C \to 1$. There holds

$$\begin{aligned} x(t) &:= \lim_{C\to 1}\frac{1}{1-C}x_C(t) \\ &= -\frac{d}{dC}[te^{-t} - C^2te^{-Ct}]_{C=1}\chi_{[0,\infty)}(t) \\ &= t(2-t)e^{-t}\chi_{[0,\infty)}(t) \ . \end{aligned} \quad (16)$$

More precisely, we have

$$\frac{1}{1-C}x_C(t) = x(t) + (1-C)te^{-t}R(t,C), \quad (17)$$

where

$$R(t,C) = -1 + (1+C)t + C^2\frac{1-(C-1)t - e^{-(C-1)t}}{(1-C)^2} \ . \quad (18)$$

Now there holds for this $R(t,C)$ that

$$R(t,C) = R(t) + \varepsilon(t) = -1 + 2t - \frac{1}{2}t^2 + \varepsilon(t) \ , \quad (19)$$

where the error $\varepsilon(t)$ is of the order $\frac{1}{6}|1-C|t^3e^{|1-C|t}$ or less. For the leading behavior R of $R(t,C)$ we have

$$\int_0^\infty te^{-t}R(t)dt = 0 \ ; \\ -1 \le R(t) \le 1 \ , \ 0 \le t \le 4 \ . \quad (20)$$

Next an overview is given, of some characteristics of $x(t)$. We compute

$$\|x\|_2^2 = \int_0^\infty (t(2-t)e^{-t})^2 dt = \frac{1}{4} \;, \tag{21}$$

$$\|x\|_1 = \int_0^\infty |t(2-t)e^{-t}| dt = \frac{8}{e^2} = 1.082682266 \;. \tag{22}$$

Furthermore, for the Fourier transform $X(\omega)$ of x we find

$$X(\omega) = \int_0^\infty e^{i\omega t} t(2-t)e^{-t} dt = \frac{-2i\omega}{(1-i\omega)^3} \;. \tag{23}$$

The spectral version of Eq. 17 and 18 reads

$$\frac{1}{1-C} X_C(\omega) = X(\omega) - 2i\omega(1-C)\frac{C - \frac{1}{2}i\omega + \frac{1}{2}\omega^2}{(1-i\omega)^3(C-i\omega)^2} \;. \tag{24}$$

The admissibility constant C_x of x is given by:

$$C_x = \int_{-\infty}^{\infty} |X(\omega)|^2 \frac{d\omega}{|\omega|} = 2 \;. \tag{25}$$

The wavelet transform of x, using x itself or the the time-reversed signal x_- as wavelet are given by

$$\begin{aligned} CWT_x[x](t,a) = \tfrac{1}{\sqrt{a}} \textstyle\int_{-\infty}^{\infty} x(\tau) x\left(\frac{t-\tau}{a}\right) d\tau = \\ \tfrac{e^{-t/a}}{a^2\sqrt{a}}[-2at(t-2)e_2(-\alpha,t) \\ +(2t^2+(8a-4)t-8a)e_3(-\alpha,t) - 12(t+a-1)e_4(-\alpha,t) \\ +24e_5(-\alpha,t)],\; t>0 \;, \end{aligned} \tag{26}$$

while $CWT_x[x](t,a) = 0$ for $t \le 0$. In Eq. 26 we have set

$$\begin{aligned} e_l(\beta,t) &= \frac{1}{\beta^l}\left(e^{\beta t} - 1 - \beta t - \ldots - \frac{(\beta t)^{l-1}}{(l-1)!}\right) \\ &= t^l \sum_{j=0}^{\infty} \frac{(\beta t)^j}{(j+l)!} \end{aligned} \tag{27}$$

which is to be read as $\frac{t^2}{l!}$ when $\beta = 0$ in accordance with the last member of Eq. 27. Also we have $\alpha = 1 - a^{-1}$ in Eq. 26. Furthermore we have

$$\begin{aligned} &CWT_{x_-}(t,a) = \frac{1}{\sqrt{a}} \int_{-\infty}^{\infty} x(\tau) x\left(\frac{\tau - t}{a}\right) d\tau = \\ &t \ge 0 \;:\; \frac{e^{-t}}{a^2\sqrt{a}}[-2a\left(\frac{a}{a+1}\right)^2 t(t-2) \\ &+\left(\frac{a}{a+1}\right)^3 (2t^2-(8a+4)t+8a) \\ &+12\left(\frac{a}{a+1}\right)^4 (t-a-1) + 24\left(\frac{a}{a+1}\right)^5] \;, \\ &t \le 0 \;:\; \frac{e^{-t/a}}{a^2\sqrt{a}}[-2a^2\left(\frac{a}{a+1}\right)^2 t(t+2a) \\ &+\left(\frac{a}{a+1}\right)^3 (2t^2+(8+4a)t+8a) \\ &-12\left(\frac{a}{a+1}\right)^4 (t+a+1) + 24\left(\frac{a}{a+1}\right)^5] \;. \end{aligned} \tag{28}$$

We finally compute the moments of x as

$$\int_0^\infty t^k x(t) dt = -(k+1)!k \;,\; k = 0,1,.. \;, \tag{29}$$

and this vanishes for $k = 0$ only.

III. Application to clinical data

Figure 2 shows three visual representations of the wavelet transform of a modelled myoclonic seizure, using x as a model and two accelerometric patterns from clinical data that are associated with a myoclonic seizure and an other movement. The wavelet used is the time reversed version of x.

For the myoclonic seizure, the coefficients with the highest

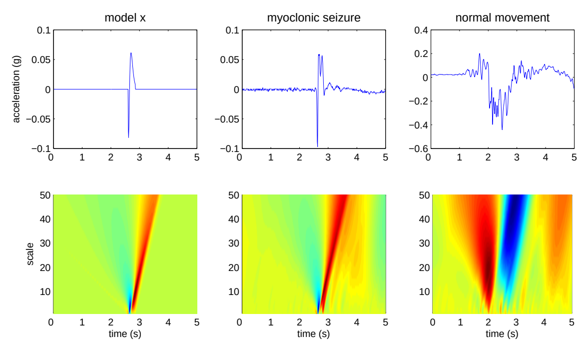

Fig. 2. Wavelet transform of x, an accelerometric pattern that is associated with a myoclonic seizure, and an accelerometric pattern that is associated with a movement that is not a myoclonic seizure.

values lie in the 2–8 range of scales. This agrees with the findings presented in [5]. Similar behavior can be observed between the modelled myoclonic seizure and the real myoclonic seizure. In the scalogram of the other movement we see high values at high scales. This example shows that it is possible to distinguish between myoclonic seizures and other movements using the wavelet presented in this paper.

IV. Comparison to other wavelets in literature

In this section, the new wavelet x, a smoothed version of x and its odd extension are compared to some wavelets described in literature.

Figure 3 shows the Cauchy wavelet and its Fourier transform [3].

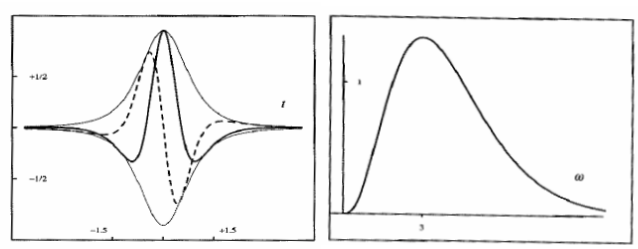

Fig. 3. Cauchy wavelet $x(t) = \frac{1}{2\pi(1-it)^3}$ (imaginary part dashed), and its Fourier transform $X(\omega) = \omega^2 e^{-\omega}$, from [3].

Figure 4 shows the Bessel wavelet and its Fourier transform [3].

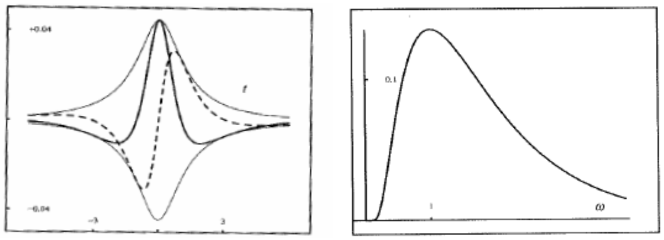

Fig. 4. Bessel wavelet $x(t) = \frac{1}{\pi\sqrt{1-it}} K_1(2\sqrt{1-it})$ (imaginary part dashed), with K_1 a modified Bessel function of order 1, and its Fourier transform $X(\omega) = e^{-(\omega+1/\omega)}$, $\omega > 0$, from [3].

Observe that x is real, causal and of simple from so that relevant data concerning x can be computed analytically. Figure 5 shows the signal $x(t)$ and its Fourier transform $|X(\omega)|$ (solid lines). It can be seen that $|X(\omega)|$ decays rather slowly, roughly like $2/\omega^2$, as $\omega \to \infty$. This is due to the abrupt rise of $x(t)$ at $t = 0$.

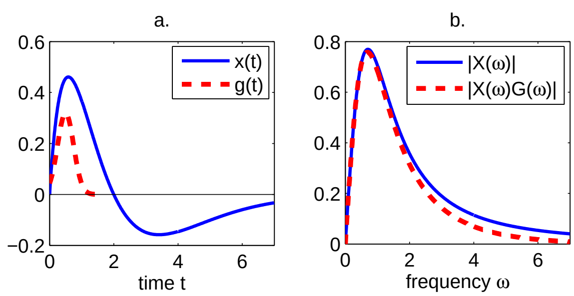

Fig. 5. a. $x(t)$ and a Gaussian window g. b. $|X(\omega)|$, and $|X(\omega)G(\omega)|$.

In Fig. 5 (a) also a Gaussian window g is depicted (dashed line) by which x(t) is to be smoothed. The resulting spectrum $|X(\omega)G(\omega)|$ is depicted in Fig. 5 (b) (dashed line) and decays quite a bit faster. Smoothing $x(t)$ with a Gaussian g yields a non-causal signal; also, it is certainly not so that a Gaussian g is optimal and/or in complete agreement with physiology.

1) Odd extension of x: A different sort of modification is obtained when we consider the odd extension of x,

$$x_{odd} = x(t) - x(-t) \ , \ t \in \mathbb{R} \ , \tag{30}$$

whose spectrum is given by

$$X_{odd}(\omega) = 2i\,Im[X(\omega)] = 4i\frac{3\omega^3 - \omega}{(1+\omega^2)^3} \ , \omega \in \mathbb{R} \ . \tag{31}$$

Fig. 6 shows $x_{odd}(t)$ and $|X_{odd}(\omega)|$. Note that x_{odd} looks quite similar to (the imaginary part) of certain wavelets that can be found in literature. Compared to $X(\omega)$, $X_{odd}(\omega)$ decays more rapidly, like $12/\omega^3$, as $\omega \to \infty$. Furthermore, $X_{odd}(\omega)$ has a peak value that is 1.5 times larger than the peak value of $X(\omega)$, and this peak value occurs at an ω that is more than 1.5 times larger than the ω at which $X(\omega)$ has its peak value.

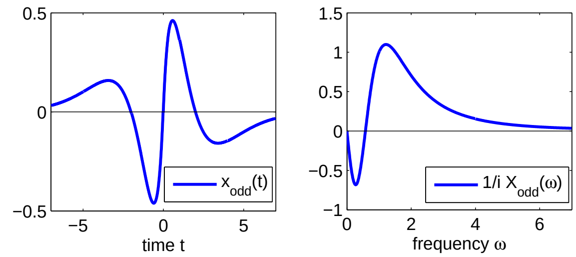

Fig. 6. $x_{odd}(t)$ and $\frac{1}{i}X_{odd}(\omega)$.

V. Conclusion

A new wavelet, based on an analytical description for accelerometric patterns associated with myoclonic seizures has been introduced. Explicit computations are feasible for the frequency response $X(\omega)$, the admissibility condition and admissibility constant, the wavelet transform of x itself using x or its time-reversed version x_- (matched filter) as analyzing wavelet. The new wavelet, a Gaussian smoothed version of it, and the odd extension of it, have similar appearances as wavelets known in literature. It is possible to distinguish between myoclonic seizures and other movements using the wavelet presented in this paper. Thus the wavelet has excellent potential in the detection of myoclonic seizures from accelerometric data of arm movements of epileptic patients.

References

[1] M. Hallett, Myoclonus: Relation to Epilepsy, *Epilepsia*, vol. 26, Suppl. 1, 1985, pp. S67–S77.

[2] T. M. E. Nijsen, R. M. Aarts, J. B. A. M. Arends, P. J. M. Cluitmans, Model for arm movements during myoclonic seizures, Proceedings of the 29th Annual International Conference of the IEEE EMBS, Cité Internationale, Lyon, France, August 23-26, 2007, pp. 1582–1585

[3] M. Holschneider, Wavelets, An Analysis Tool, Clarendon Press, Oxford, 1995.

[4] I. Daubechies, Ten Lectures on Wavelets, SIAM, Philadelphia, 1992.

[5] T. M. E. Nijsen, P. J. M. Cluitmans, R. M. Aarts, P. A. M. Griep, Short time Fourier and wavelet transform for accelerometric detection of myoclonic seizures, IEEE/EMBS Benelux, 7-8 December 2006, Brussels.